Coherent scatter from radar aurora: assessment of the precision and spatiotemporal variability of estimations

Enrique Rojas David Hysell

Cornell University

Abstract

The **main goal** of this work is to *evaluate the precision of the estimation of convection patterns measured with our coherent radar system. We are also exploring the relation between active events and the dispersion of the electric field estimates.*

I. Introduction

Radar aurora can be studied with high precision and spatiotemporal resolution using small coherent radars. This systems can measure echoes from irregularities in the plasma, which are related with other physical parameters of the plasma, through known models.

The radar we use is a 30MHz coherent scatter radar imager located in Homer, Alaska. Figure 2 shows a plot of the estimated spectral moments combined with auroral optical data in the background. The system has a resolution of 2.25km and 0.5° in range and azimuth respectively. The radar detects echoes from 5m wavelength irregularities, which are processed to produce the spectral moments of the signal.

The estimations of doppler (ω_d) and spectral width ($\Delta\omega_d$) are then used to calculate convection patterns, (Figure 1). The doppler data is related to the convection field $\vec{V}_d$ through a heuristic relation [1], from this we can estimate a smooth potential that minimize discrepancies with the data.

In this work, we will show the preliminary results of the use of this method to investigate the event of December 20, 2015. The region of interest will be the one enclosed inside the polar sector defined by the dashed lines in Figure 2.

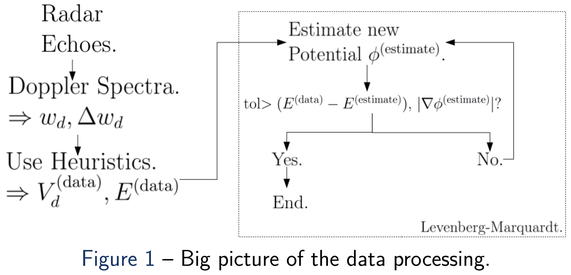

Figure 1 – Big picture of the data processing.

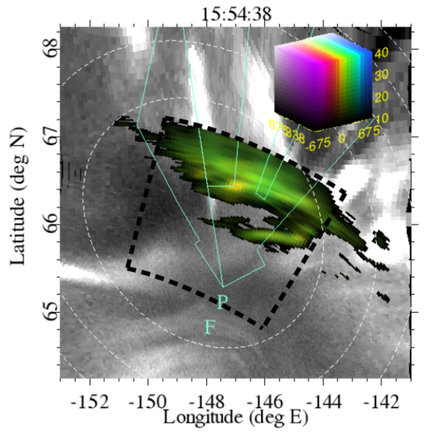

Figure 2 – Doppler velocities (hue), SNR (brightness) and spectral width (saturation).

II. Heuristics and Inversion Method

We can attempt to infer the transverse electric field wherever coherent scatter data are available using the empirical relations:

$$\omega_d = \left(350 + \left[\frac{V_d}{100}\right]^2\right)\cos(\theta - \theta_0) + \nu_i \qquad (1)$$

$$\Delta\omega_d = 0.5\left(350 + \left(\frac{V_d}{100}\right)^2\right)|\sin(\theta - \theta_0)| \qquad (2)$$

where V_d is the convection speed, θ the flow angle and θ_0 a correction term to account for wave turning effects while ν_i models the influence of neutral winds. If we call $\phi^{(data)}$ to the potential calculated in each point from the data $V_d^{(data)}$ and $\theta^{(data)}$, the equation to get the convection patterns will be:

$$\phi^{(est)} = \min_{\phi} |\vec{V}_d^{(data)} - \vec{V}_d(\phi)| + \beta|\nabla\phi| \qquad (3)$$

where β is an optimization parameter. Eqn (3) is solved with the Levenberg–Marquardt method.

III. Estimation of Flows

The flows and potential estimated for the Figure 2 is shown in Figure 3. Although the polar sector is being shown in a rectangular grid, the quantities are defined in cylindrical coordinates at each point.

Because $\vec{V}_d \propto \vec{E} \times \vec{B}$, the quasistatic nature of the problem makes $\nabla \cdot \vec{V}_d = 0$. This means that the flows estimated directly from the data, must also be close to incompressibility.

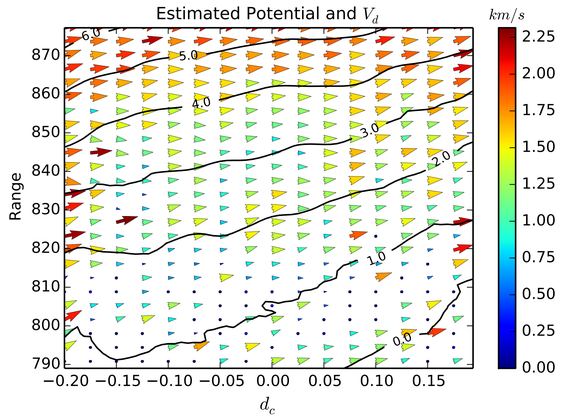

Figure 3 – Estimated convection velocity field $\vec{V}_d$ and potential.

Figure 4 shows the divergence field scaled by a factor $F^{(est)}$:

$$\frac{1}{F^{(est)}} = \frac{1}{dr}\sqrt{\frac{1}{2}\left(\vec{V}_d^{(data)} - \vec{V}_d^{(est)}\right)^2} \qquad (4)$$

where dr is the radial step. In other words, $|\nabla \cdot \vec{V}_d^{(data)}|F^{(est)}$ scale the divergence of the data with respect to a rough estimate of the flux across grid cells.

Because of the geometry of the problem, $|\nabla \times \vec{V}_d| = \nabla^2\phi$. This implies that the tendency to rotate of the flows is related to the inhomogeneities of the system. Without any model of how the curl relates with the plasma structure is very difficult to understand the values of $|\nabla \times \vec{V}_d|$, so Figure 5 is normalized with the maximum value of the curl, to appreciate the distribution and how it relates the rotation of the flow vectors.

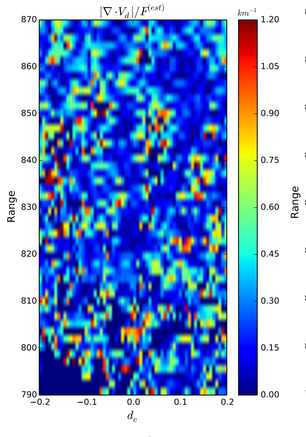

Figure 4 – Scaled div.

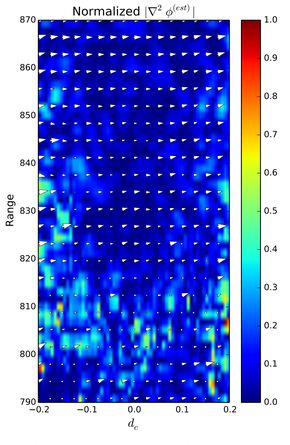

Figure 5 – Normalized rot.

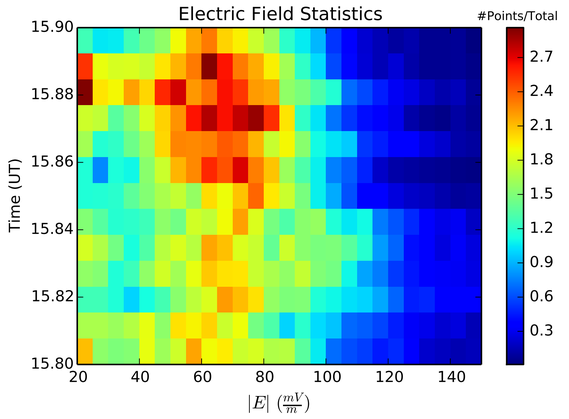

Figure 6 – Each row shows an histogram of the spatial distribution of $\vec{E}^{(est)}$.

Figure 6 shows the spatial distribution of electric field estimations from $\phi^{(est)}$. The dispersion of $|\vec{E}|$ consistently maps to events of higher geomagnetic activity and flows with higher peaks. This type of information may be useful to inform the assumptions of homogeneity of some large scales models.

IV. Discusion and Future Work

We were able to make a coarse assessment of the inversion results by means of the expected properties of the plasma. The definitive way to do it is through a careful error analysis. In future work, we will compare the flow derivatives with the expected propagated error.

Conclusions

- Coherent radars produce high resolution reconstructions of convection fields.
- Properties of the fields give insight about the reconstruction effectiveness.
- Next step: propagate errors across model + compare them to vector field estimates.

References

[1] Hysell, D., R. Miceli, J. Munk, D. Hampton, C. Heinselman, M. Nicolls, S. Powell, K. Lynch, and M. Lessard, Comparing VHF coherent scatter from the radar aurora with incoherent scatter and all–sky auroral imagery, *J. Geophys. Res.*, *117*, A10313, 2012.